

EUROPEAN ORGANIZATION FOR NUCLEAR RESEARCH

Proposal to the ISOLDE and Neutron Time-of-Flight Committee

Charge and spin states of Fe in binary compounds

[submission date: 22/9]

H. P. Gunnlaugsson¹, L. Hemmingsen², H. Masenda³, S. Olafsson¹, S. K. Dedushenko⁴, A. Gerami⁵, J. Schell⁶, D. Zyabkin⁷, K. Bharuth-Ram⁸, The Mössbauer collaboration at ISOLDE/CERN⁹

¹Science Institute, University of Iceland, Iceland; ²Department of chemistry, University of Copenhagen, Denmark; ³School of Physics, University of the Witwatersrand, South Africa; ⁴Department of Chemistry, Moscow State University, Moscow, Russia; ⁵Department of Physics, K.N. Toosi University of Technology, Tehran, Iran; ⁶ISOLDE, CERN, Geneva, Switzerland; ⁷TU Ilmenau, Ilmenau, Germany; ⁸School of Physics, University of KwaZulu-Natal, Durban, South Africa ⁹<https://e-ms.web.cern.ch/content/collaborators>

Spokesperson(s): H. P. Gunnlaugsson & L. Hemmingsen
Local contact: J. Schell

Abstract

We propose to measure, with emission Mössbauer spectroscopy, the electron density at the nucleus with monopole interaction (isomer shift) of ⁵⁷Fe probe nuclei in binary compounds. The results will add to existing data on electron densities at the ⁵⁷Fe nucleus for different Fe spin/charge states and aid in the development of a semi-empirical model which takes into account (amongst others) electronegativities and nearest neighbour distances to predict isomer-shifts for different charge/spin configurations of Fe in binary compounds. Such a model will allow for determination of unknown charge/spin states of Fe impurities and compounds from Mössbauer spectroscopy studies.

Requested shifts: 12 shifts, (split into ~3 runs over ~3 years)



1 INTRODUCTION

The isomer shift in Mössbauer spectroscopy (MS), δ_{RT} , is related to the electron density at the nucleus, $|\psi(0)|^2$, as (see e.g. [1] and references therein)

$$\delta_{RT} = -\alpha(|\psi(0)|^2 - C)$$

where α is a constant determined from comparison of experimental and theoretical isomer shift values ($-0.29 \text{ mm}/(s \cdot a_0^3)$ for ^{57}Fe [2]) related to the size difference of the nucleus in the excited and ground states, and C is a constant which depends on the choice of isomer shift reference scale. This quantity cannot be obtained by any of the other techniques used for measuring hyperfine interactions in solids, including Nuclear Magnetic Resonance (NMR) and Perturbed Angular Correlations (PAC). Experimentally the isomer shift is determined as the central position of a spectral component in the Mössbauer spectra with respect to the reference scale (usually metallic iron for ^{57}Fe MS).

For ^{57}Fe , the s -electrons which contribute to the electron density at the nucleus are shielded from the nucleus by $3d$ electrons. The isomer shift, hence, depends on the number (charge state) and configuration (spin state) of the $3d$ electrons.

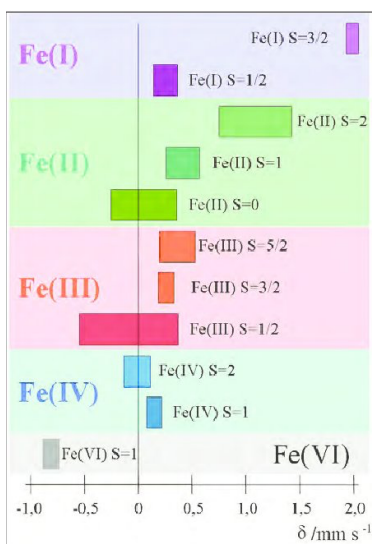


Fig. 1: Ranges of isomer shift values expected for different oxidation and spin states of iron compounds. Original version is from [3]. This version is a slight modification with recent data from [1].

Experimentally, the ranges of isomer shift values have been determined for different charge/spin states of iron compounds; the currently adopted picture is shown in Fig. 1. The ranges of isomer shifts for different charge/spin states overlap, which can make it impossible to determine uniquely charge/spin state from the isomer shift alone, except for some special cases. However, based on the knowledge of the system under study, certain charge or spin-states can be excluded, making the diagram in Fig. 1 useful.

The diagram in Fig. 1 is for ionic compounds. In the case of different degrees of covalency, the ranges of isomer shifts overlap more which completely negates the usefulness of this diagram.

1.1 Empirical model

Gunnlaugsson and Masenda [4] reported a trend of isomer shifts from covalent to ionic high-spin dilute Fe^{2+} impurities in binary compounds (based mostly on data obtained by $^{57}\text{Mn} \rightarrow ^{57}\text{Fe}$ emission Mössbauer Spectroscopy (eMS) at ISOLDE/CERN from many different experiments), c.f. Fig. 2.

The nice results obtained (Fig. 2) motivated the interest to see whether a similar trend could be found for higher electronegativity difference ($\Delta\chi_P > 2$) and for other spin/charge states. Literature data for dilute high-spin Fe^{2+} impurities in compounds with $\Delta\chi_P > 2$ were found to not follow the trend shown in Fig. 2 (see discussion in [4]) and practically no reliable data exists on other charge/spin states (Fe^{1+} is generally not assumed to be stable in simple crystals).

To investigate this lack of trend for $\Delta\chi_P > 2$ and whether the eMS using implantation of ^{57}Mn ($T_{1/2} = 1.45 \text{ min.}$) would be a reliable way to experimentally obtain more data, some compounds were investigated ‘opportunistically’ during the 2018 Mn beam-time. The data obtained (listed in Table 1, together with literature data) has resulted in a preliminary model [5] presented in Fig. 3.

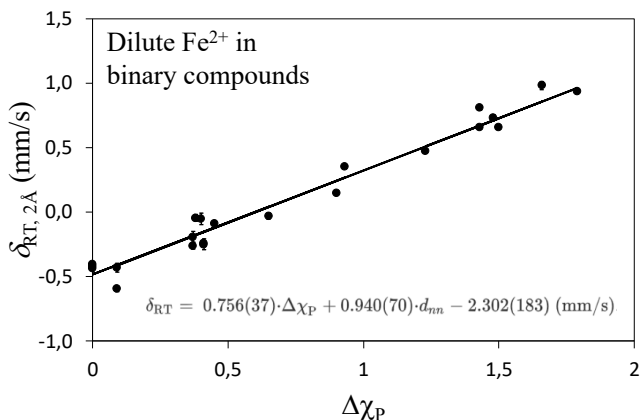


Fig. 2: Isomer shift of high-spin Fe^{2+} in dilute binary compounds (adapted from [4]). Isomer shifts (y-axis) are calculated as expected for 2 Å nearest neighbour distances, vs. difference in (Pauling) electronegativity of host atoms.

For electronegativity difference $\Delta\chi_P < 2$ the model was found to describe the isomer shifts of covalent compounds quite accurately, illustrating its usefulness in predicting the isomer shift in similar systems [4].

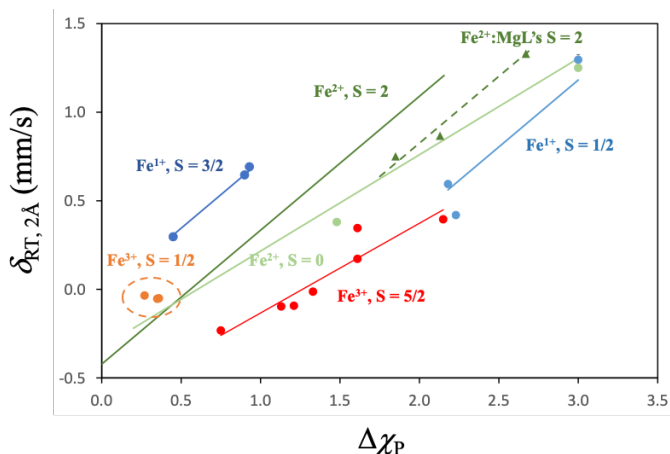


Fig. 3: Model of isomer-shifts (calculated as expected for 2 Å nearest neighbour distances) as a function of difference in (Pauling) electronegativity of host atoms for dilute Fe impurities in binary compounds. Data for six coordinated covalent Fe^{3+} compounds included for comparison.

The results were very encouraging. Not only was the eMS technique found to be effective in determining the isomer shifts of the isolated Fe atoms, it was also successful in determining the hyperfine parameters of Fe associated with point defects in the compounds [5, 6]. From the data obtained the lack of trend for $\Delta\chi_P > 2$ from (at least some of) the literature data was resolved with new charge/spin state assignments.

The trends described in Fig. 3 and Table 1 must be considered to be preliminary. Once Fig. 3 and Table 1 are populated with more data on isomer shifts of different spin/charge states, a semi-empirical model should emerge which will provide a direct method to determine spin/charge states from isomer shift values.

Table 1: List of materials/references behind the data in Fig. 3

Charge	Spin	Description
2+	2	Follows a simple trend [4] with Mg compounds plotted a bit lower (data from [7-9]), possibly evidencing atomic size effects.
	1	The only data point here is from assuming S=1 spin state for Fe^{2+} in CaF_2 . [7, 9-11]. Normally one would assume S=2 spin state for F^- ligands as these are at the start of the spectrochemical series. However, this interpretation is consistent with

	0	the low spin state of Fe in LiF [6] and may suggest that the spectrochemical series is not applicable for determining spin states of Fe in binary compounds. The trend published by Nishihara et al., [12] extended to Fe ²⁺ - Fe _I in LiF [6] and consistent with the Fe _x component observed in ⁵⁷ Mn- ⁵⁷ Fe eMS measurements in SnO ₂ [7, 13].
1+	3/2	The trend follows the data obtained on metastable Fe ¹⁺ in sulphides obtained due to after-effects in ⁵⁷ Co doped samples (see [14] and references therein)
	1/2	The trend based on data for Fe in NaCl and LiF [6] and LiCl [15]. This charge state is observed despite the general assumption that Fe ¹⁺ is not stable in simple crystals.

2 EXPERIMENTAL PLAN

2.1 Science goals

Generally, we want to use inductive reasoning to:

(a) Determine more accurately the trends proposed in Fig. 3:

For Fe¹⁺ and Fe²⁺ in the S = 0 & 1 spin states, there are too few datapoints in Fig. 3 to determine accurately both the dependence of the isomer shift on the nearest neighbour distance (d_{nn}) and on the difference in electronegativity ($\Delta\chi_p$) simultaneously, therefore more data is required. When these trends are established accurately, one can start to determine how different orbitals shield the nucleus from 3d electrons.

(b) Determine the next correction parameters. This includes (but is not limited to):

a. Dependence of isomer shift on coordination number and geometry.

There should be a dependence on coordination number (as exists for high spin Fe³⁺), however, it is unclear how automatic correction for this effect exists in compounds with low d_{nn} and low coordination number. So far, it has been sufficient to make use of the average d_{nn} , which is obviously wrong, but more data is required.

b. Dependence of isomer shift on atomic sizes.

Data obtained on Fe replacing Mg in high spin (S = 2) Fe²⁺ compounds shows shifts toward lower $\delta_{RT,2A}$ values (cf. Fig. 3). This could indicate atomic sizes dependence. More data is required to determine how this correction should be applied.

c. Nonlinear dependence of isomer shift on d_{nn} .

For the data obtained so far, a linear approximation of the dependence of the isomer shift on d_{nn} is sufficient, but measurements of more extreme cases are required to establish better models.

2.1.1 Outlook

When the scientific goals have been met, we will have established a method to determine the charge/spin state of Fe in binary compounds. In the succeeding steps, this study can be extended to more complicated systems:

a) Data obtained by the eMS collaboration [7] on compounds with more than two elements follow the preliminary trends presented in Fig. 3. As more data is obtained on different systems (fx. (In, Al, Ga)N's [16]), it is envisioned that this will aid to document the isomer shift vs. spin/charge state trends for more general systems than binary compounds.

b) Based on selected literature data, the preliminary trends observed here also appear to apply to complexes with "almost" regular octahedral and tetrahedral symmetries. With better modelling

on the dependence of isomer shift on the coordination number and geometry, the model can be extended to Fe complexes.

With reliable trends for different charge/spin states, one can start to derive new estimates of the isomer shifts of high Fe charge states making use of materials with cations in higher charge states than conventionally observed for Fe.

The data obtained so far, seems to indicate that the well-known spectrochemical series can not reliably predict high/low spin configurations of Fe. More data is required to resolve this dilemma.

2.2 Samples

Binary compounds with high electronegativity difference ($\Delta\chi > 2$) are obtained from selection of positive (metal) ions from the groups 1 (M^{1+}) and 2 (M^{2+}) with negative (ligand) ions from group 15 (L^{3-}), 16 (L^{2-}) and 17 (L^{1-}) in charge neutral ratios. This gives >100 possible compounds to select from. Only few are available as single crystals, but most are commercially available as anhydrous powder or can be easily prepared as powders using simple chemical reactions. We have started the development of a sample holder to measure powder samples on tilted heaters (see below) although other options exist for some compounds. Table 2 lists the type of compounds that will be investigated in this study.

Table 2: Possible compounds to use for this study. Compounds of the type $M_3^{1+}L^{3-}$ and $M_3^{2+}L_2^{3-}$ are not considered in this table. The table lists the number of compositions already studied and the number needed for a full study.

Configuration	Types of hosts	Examples	Compositions studied/needed
$Fe^{2+}, S = 0$	Octahedral crystal field. Amongst them are rock-salt & rutile structures.	MgS; (Ca, Sr, Ba)(O, S, Se, Te) & Mg(Cl ₂ , Br ₂ , I ₂), ...	2/5
$Fe^{2+}, S = 1$	Tetrahedral crystal field. Amongst them are fluorite and Zink-blende structures.	CaF ₂ , SrF ₂ , SrCl ₂ , BeF ₂ , Be(O, S, Se, Te) ...	1/6
$Fe^{2+}, S = 2$	Compositions listed above with low crystal field. Also low $\Delta\chi_F$ compounds and compounds with cations from transition metals and nonmetal columns of the periodic system	Mg(O, F ₂) and see also [4]. Obvious candidates include Ag(F - I), CuI, (Zn-Hg)O	22/5
$Fe^{1+}, S = 1/2$	Octahedral crystal field. Rock salt structure	(Li, Na, K, Rb)(F, Cl, Br, I) & CsF.	3/4
$Fe^{1+}, S = 3/2$	Tetrahedral crystal field, anti-fluorite & CsCl structures	(Li, Na, K, ...) ₂ (O, S, Se, ...) most anti-fluorite structure & Cs(Cl, Br, I)	3/4

Additionally, compounds with high-valent elements (OsO₄/RuO₄, Re₂O₇/ & CrO₃) will be tested to make use of the new physics that will emerge from the proposal.

2.2.1 Additional equipment for eMS

Powder samples are not ideal to work with by implantation of horizontal beams. This requires installation of tilted sample holders equipped with heaters where the sample can be held at angles $<35^\circ$. These will be installed on an additional lid on the implantation chamber [17].

2.3 eMS characterization

The main characterization technique is ^{57}Fe emission Mössbauer spectroscopy following implantation of ^{57}Mn ($T_{1/2} = 1.45$ min.). The samples are held in a multi-purpose implantation chamber and the 14.4 keV radiation is measured with a resonance detector equipped with ^{57}Fe in a stainless steel electrode mounted on a conventional Mössbauer drive system outside the implantation chamber.

Mössbauer spectroscopy gives the required parameter $|\psi(0)|^2$ from experimental determination of δ_{RT} , and additionally many other quantities of importance in the determination of the spin/charge state. These include:

- The relative intensity of the spectrum which is related to the Debye-Waller factor: If Mn/Fe cannot enter regular lattice sites and reside on interstitial or damage sites, these are sites of low Debye-Waller factor. This is observed to be the case in BaF_2 , where only broad low intensity lines are observed [7].
- Quadrupole splitting of spectral components: originates from the orbital population and site symmetry of the probe nuclei: In non-cubic environments, quadrupole splitting originates from lattice contribution (temperature independent) or from non-equal population of orbitals (temperature dependent). Some defect-site hypotheses can be excluded/identified by monitoring this parameter.
- Line-width: Variations in the local environment of the probe. fx. damage sites = probes in heavily damaged zones due to the implantation damage show broadening.
- Temperature dependent site populations: Some sites, fx. damage sites, show less intensity with increased temperature due to thermally activated annealing, while some defect sites, caused by trapping of highly mobile defects created in the annealing can increase in intensity. Metastable defect sites can disappear at elevated temperatures.

There are two main properties of eMS using ^{57}Mn make it superior to conventional Mössbauer spectroscopy (MS) using doped samples:

- (1) The concentration required ($<10^{-3}$ at.%) is a fraction of what is required for MS (~ 0.1 at.%) and
- (2) the timescale of the experiments is minutes with eMS compared to days with MS.

Both these properties eliminate the possibility of precipitation and one can safely assume that the Mn/Fe is dilute in the samples. With the truly dilute Mn/Fe concentrations in the sample, common defect structures including high-spin Fe^{3+} , are easily distinguished as they show slow paramagnetic relaxations.

For each sample composition, a temperature series of measurements will be required (i.e. measurement at 6-7 different implantation/measurement temperatures). For specific cases, isothermal annealing studies using so-called time delayed measurements [18] may be required.

Post characterization of samples is not required a priori. However, should the eMS spectra reveal evidence of nonstoichiometry, the effects of heating can be simulated for post-characterization (XRD) of samples. Some compounds are hygroscopic. High degree of hydration can be detected by IR-spectroscopy or coulometric Karl-Fischer titration in some cases (e.g. for surface water in powders).

2.4 Additional characterization

In some cases, it may be of interest to post-characterize samples, and within the Mössbauer collaboration we have access to wide range of relevant characterization techniques including EPR, MS using stable ^{57}Fe in samples and XRD.

2.5 Theory

With theoretical calculation of hyperfine parameters, such as the isomer shift (δ) and quadrupole splitting (ΔE_Q) it is possible to obtain additional confidence on site assignments and test hypothesis on the dependence of hyperfine parameters on structural variations.

Packages for calculations include the WIEN2k package. It performs quantum mechanical calculations on periodic solids using the full-potential (linearized) augmented plane-wave and local-orbitals [FP-(L)APW+lo] basis set to solve the Kohn–Sham equations of density functional theory [ref1]. The package includes routines specifically for the determination of Mössbauer parameters [2, 19-21].

3 CONCLUSIONS/OUTLOOK

The proposal outlined here aims at determining Mössbauer isomer shifts of unusual charge/spin states of Fe in binary compounds with a range of electronegativity differences. The results will give additional experimental information on how the $3d$ electrons shields the nucleus from the s-electrons.

Experimentally determined isomer shifts together with theory will be used to develop semi-empirical models that can be used to determine unknown charge/spin states of Fe in materials from isomer shift measurements.

For high spin Fe^{2+} , it has been determined that the isomer shift is predominantly determined from nearest neighbour distances and difference in electronegativity of the host atoms. We will investigate experimentally how other factors such as atomic size, coordination number, crystal symmetry, ligand chemistry etc. affect the charge/spin state of Fe.

Summary of requested shifts:

A temperature series of measurements (i.e. measurements at different temperatures in the range 300-700 K) will be conducted for each sample composition. In specific cases isochronal annealing studies can be employed using so-called time-delayed measurements [18], or, if required, low temperature measurements may be undertaken for testing hypotheses.

On the average, temperature series for each composition requires about two hours, taking into account sample changes. Time-delayed measurements (TDM) may require about an hour, and our rough estimate is that one TDM per composition is required.

It is estimated that 24 compositions are needed for a full study (+ compounds with highly valent elements). Including increments of 20% for contingency/opportunistic science and 10% for calibration adds up to a total of 13 shifts that are needed.

Beam	Min. Intensity	Min. Energy	Target/ion source	Shifts
^{57}Mn	$3 \cdot 10^8$ ions/s	50 keV	UC ₂ /RILIS	13

References:

1. P. Gülich, E. Bill and A. X. Trautwein, Mössbauer Spectroscopy and Transition Metal Chemistry, Springer-Verlag Berlin Heidelberg (2011), doi.: 10.1007/978-3-540-88428-6
2. U. D. Wdowik and K. Ruebenbauer, "Calibration of the isomer shift for the 14.4-keV transition in Fe57 using the full-potential linearized augmented plane-wave method," Phys. Rev. B, vol. 76, p. 155118, 2007
3. N. N. Greenwood, T. C. Gibb, Mössbauer Spectroscopy. Chapman and Hall, London (1971)
4. H. P. Gunnlaugsson, H. Masenda, Mössbauer isomer-shift of ferrous iron impurities in ionic and covalent binary compounds, J. Phys. Chem. Solids, 129 (2019) 151-154, doi.: 10.1016/j.jpcs.2018.12.037.
5. H. P. Gunnlaugsson, presentations at the Workshop of the applications of Emission Mössbauer Spectroscopy, Bilbao, 2019.
6. H. P. Gunnlaugsson et al., Charge and spin state of Fe in NaCl and LiF, Manuscript in preparation (2020) [available upon request]
7. Mössbauer collaboration at ISOLDE/CERN, unpublished data.
8. T. E. Møhlolt, R. Mantovan, H. P. Gunnlaugsson, A. Svane, H. Masenda, D. Naidoo, K. Bharuth-Ram, M. Fanciulli, H. P. Gislason, K. Johnston, G. Langouche, S. Ólafsson, R. Sielemann, G. Weyer, and the ISOLDE Collaboration, Interstitial Fe in MgO, J. Appl. Phys. 115 (2014) 023508, <http://dx.doi.org/10.1063/1.4861403>
9. A. Cruset, J. M. Friedt, Stabilization of aliovalent ions observed by Mössbauer emission spectroscopy in 57Co-doped simple ligand compounds, phys. stat. sol. (b), 47 (1971) 655-662, doi.: 10.1002/pssb.2220470230
10. J. R. Regnard and J. Pelzl, Isomer Shift of Multiple Charge States of Iron in CaO and CaF₂. phys. stat. sol. (b) 56 (1973) 281
11. C. Garcin, P. Imbert, G. Jéhanno, J. R. Régnard, G. Férey, M. Leblanc and A. Gerard, Mössbauer absorption and emission experiments in CaF₂(57Fe): relaxation and after-effect study, J. Physique 47 (1986) 1977-1988.
12. Y. Nishihara and S. Ogawa, Mössbauer study of 57Fe in the pyrite-type dichalcogenides, The Journal of Chemical Physics 71 (1979) 3796-3801, doi: 10.1063/1.438787
13. H. P. Gunnlaugsson, K. Nomura, T. E. Møhlolt, S. Shayestehaminzadeh, K. Johnston, R. Mantovan, H. Masenda, M. Ncube, K-Bharuth Ram, H. Gislason, G. Langouche, D. Naidoo, S. Ólafsson, G. Weyer, the ISOLDE Collaboration, Characterization of Fe States in Dilute 57Mn implanted SnO₂, Hyp. Interact. 226(2014) 389-396, <http://dx.doi.org/10.1007/s10751-013-0936-0>
14. T. Becze-Deák, L. Bottyán, D.L. Nagy, U. W. Pohl and H. Spiering, On the applicability of the model of competing acceptors to Fe¹⁺ in 57Co:ZnSe, Hyperfine Interactions volume 126, pages115–119(2000), doi.: 10.1023/A:1012696829127
15. N. Kai, Mössbauer Spectroscopy Study of Alkali Chloride Crystals Containing a Small Amount of Iron (II), The Journal of Shimonoseki University of Fisheries, 30 (1981) 63-81
16. H. Masenda, H. P. Gunnlaugsson, D. Naidoo, K. Bharuth-Ram, R. Mantovan, H. P. Gislason, A. Bonanni, A. Tarazaga, A. Vantomme, K. Johnston, J. Schell, B. Qi, S. Ólafsson, Lattice sites, charge and spin states of Fe in In_xGa_{1-x}N studied with emission Mössbauer spectroscopy, Proposal to the ISOLDE and Neutron Time-of-Flight Committee (2016), <https://cds.cern.ch/record/2222331/files/INTC-P-485.pdf>
17. D. V. Zyabkin et al., Nucl. Instruments Methods Phys. Res. Sect. A. 968, 163973 (2020), <https://doi.org/10.1016/j.nima.2020.163973>

18. H. P. Gunnlaugsson, G. Weyer, R. Mantovan, D. Naidoo, R. Sielemann, K. Bharuth-Ram, M. Fanciulli, K. Johnston, S. Olafsson, G. Langouche, Isothermal defect annealing in semiconductors investigated by time-delayed Mössbauer spectroscopy: application to ZnO, *Hyperfine Interact.* 188 (2009) 85–89, <http://dx.doi.org/10.1007/s10751-008-9893-4>
19. P. Blaha, K. Schwarz, G. K. H. Madsen and D. Kvasnicka, WIEN2k, An Augmented Plane Wave + Local Orbitals Program for Calculating Crystal Properties, Austria (2001, Karlheinz Schwarz: Techn. Universität Wien, 2001.
20. F. Neese, Prediction and interpretation of the ^{57}Fe isomer shift in Mössbauer spectra by density functional theory, *Inorganica Chimica Acta*, 337 (2002) 181 - 192, doi.: 10.1016/S0020-1693(02)01031-9
21. P. Dufek, P. Blaha and K. Schwarz, “Determination of the Nuclear Quadrupole Moment of ^{57}Fe ,” *Phys. Rev. Lett.*, vol. 75, pp. 3545-3548, 1995.

Appendix

DESCRIPTION OF THE PROPOSED EXPERIMENT

The experimental setup comprises: *(name the fixed-ISOLDE installations, as well as flexible elements of the experiment)*

Part of the Choose an item.	Availability	Design and manufacturing
SSP-GLM chamber	<input checked="" type="checkbox"/> Existing	<input checked="" type="checkbox"/> To be used without any modification
Mössbauer set-up (eMIL) and Mössbauer magnetic analyser (eMMA)	<input checked="" type="checkbox"/> Existing <input type="checkbox"/> New	<input checked="" type="checkbox"/> To be used without any modification <input type="checkbox"/> To be modified <input type="checkbox"/> Standard equipment supplied by a manufacturer <input checked="" type="checkbox"/> CERN/collaboration responsible for the design and/or manufacturing
Existing equipment in the SSP lab in building 508	<input checked="" type="checkbox"/> Existing <input type="checkbox"/> New	<input checked="" type="checkbox"/> To be used without any modification <input type="checkbox"/> To be modified <input type="checkbox"/> Standard equipment supplied by a manufacturer <input type="checkbox"/> CERN/collaboration responsible for the design and/or manufacturing
[insert lines if needed]		

HAZARDS GENERATED BY THE EXPERIMENT

(if using fixed installation) Hazards named in the document relevant for the fixed [COLLAPS, CRIS, ISOLTRAP, MINIBALL + only CD, MINIBALL + T-REX, NICOLE, SSP-GLM chamber, SSP-GHM chamber, or WITCH] installation.

Additional hazards:

Hazards		
	Collection chamber and GLM beam line (SSP)	Mössbauer chamber at GLM beam line (SSP)
Thermodynamic and fluidic		

Pressure			
Vacuum	typically, 10 ⁻⁶ mbar	typically, 10 ⁻⁶ mbar	
Temperature	RT	RT – 700K	
Heat transfer			
Thermal properties of materials			
Cryogenic fluid			
Electrical and electromagnetic			
Electricity		12 V, max. 5 A sample heating during measurements	
Static electricity			
Magnetic field	[
Batteries	<input type="checkbox"/>		
Capacitors	<input type="checkbox"/>		
Ionizing radiation			
Target material			
Beam particle type (e, p, ions, etc.)		ions	
Beam intensity		10 ¹¹ ions/s	
Beam energy			
Cooling liquids	[liquid]		
Gases	[gas]		
Calibration sources:	<input type="checkbox"/>		
• Open source	<input type="checkbox"/>		
• Sealed source	<input type="checkbox"/> [ISO standard]		
• Isotope			
• Activity			
Use of activated material:			
• Description	<input type="checkbox"/> Collection in the chamber, removal from the chamber and transport to building 508	Measurement on-line with sample in the chamber	
• Dose rate on contact and in 10 cm distance		max. 0.5 μSv/h	
• Isotope		⁵⁷ Mn	
• Activity		max. 3-4 MBq per sample	
Non-ionizing radiation			
Laser			
UV light			
Microwaves (300MHz-30 GHz)			
Radiofrequency (1-300MHz)			
Chemical			
Toxic			
Harmful			
CMR (carcinogens, mutagens and substances toxic to reproduction)			
Corrosive			

Irritant			
Flammable			
Oxidizing			
Explosiveness			
Asphyxiant			
Dangerous for the environment			
Mechanical			
Physical impact or mechanical energy (moving parts)			
Mechanical properties (Sharp, rough, slippery)			
Vibration			
Vehicles and Means of Transport			
Noise			
Frequency			
Intensity			
Physical			
Confined spaces			
High workplaces			
Access to high workplaces			
Obstructions in passageways			
Manual handling			
Poor ergonomics			

0.1 Hazard identification

3.2 Average electrical power requirements (excluding fixed ISOLDE-installation mentioned above): *(make a rough estimate of the total power consumption of the additional equipment used in the experiment)*